J. Fluid Mech. (1965), *vol.* **23** *part* 2, *pp.* 373–384
Printed in Great Britain

An experimental determination of the slow motion of a sphere in a rotating, viscous fluid

By T. MAXWORTHY

Jet Propulsion Laboratory, California Institute of Technology

(Received 15 January 1965)

The drag of a sphere has been measured as it moves along the axis of a rotating, viscous fluid. Rotation has been found to modify the classical low-Reynolds-number flow so that the drag is increased and the effects of finite Reynolds number, R, and of wall proximity are reduced as the rotation parameter, the Taylor number T, increases. The results confirm the theory of Childress (1963, 1964) when both Reynolds number and Taylor number are small. The rate at which the sphere rotates with respect to the rotating fluid frame has also been measured and was found to be less than the values calculated by Childress (1964) for small T and R, but to approach the theoretical values in a reasonable way.

1. Introduction

Fluid motions at low Reynolds numbers have received attention during the past several years. Theoretical attempts have been made to extend the range of R over which accurate comparison to the real flow can be made. Recent experimental work (Maxworthy 1965) suggests that higher order terms in the asymptotic series obtained for sphere drag, for example, may not be a very significant improvement over the first-order correction.

In the present work we add another externally controllable force to the equations of motion in order to study further the balance between the various terms and check the usefulness of the asymptotic analyses. If a body is allowed to move in a fluid rotating with solid body rotation, two extra forces are introduced: the force caused by centripetal acceleration, and the Coriolis force. The former is readily assimilated into the pressure-gradient term of the equation of motion (Squire 1956), and only the latter need be included separately since density gradients in the flow are not considered.

Specifically, the theory of Childress (1964) is for small Taylor number T and small Reynolds number R, where $T = \Omega a^2/\nu$, $R = Ua/\nu$, Ω is the angular velocity of the basic solid-body rotation, U and a are the sphere velocity and radius, respectively, and ν is the kinematic viscosity. It is possible to measure accurately the quantities of interest in this case in order to resolve such questions as: What is meant by small? What happens when T and R are large? What balance exists between the inertia, the Coriolis and the viscous forces in the flow? Can the effect of one be changed by changing externally the value of another? The answers

should indicate a great deal about the nature of the equations and the solutions obtained.

Subsidiary, but related, questions concerning the effect of wall proximity and its modification by rotation are also important. Answers have been obtained to all of these questions and, hopefully, will make it possible to obtain limits of theoretical applicability in problems which are not amenable to simple and direct experimental check.

The most important of these problems, and in fact the one which prompted the present investigation, is the slow flow of an electrically conducting fluid around a body in the presence of an aligned magnetic field. Further amplification of this point is relegated to §6·1, where the similarity between magneto-fluid dynamics and the dynamics of rotating fluids is developed, and the present results are considered in the light of the similarity.

2. A brief description of the experimental technique

In order to avoid future confusion, the most important piece of nomenclature will be introduced at this point. It is necessary to distinguish four velocities at which the test sphere moves through the fluid: (1) the velocity in a rotating fluid of finite extent, U; (2) in a rotating fluid of infinite extent, U'; (3) in a non-rotating fluid of finite extent, U_0; and (4) in a non-rotating fluid of infinite extent, U_0'.

When a sphere rises at constant velocity U_0', and low Reynolds number, $R_0' = U_0'a/\nu$, in a non-rotating medium of infinite extent, its drag, D, can be found from the experimental results of Maxworthy (1965). Since all of the forces acting upon it are in equilibrium, the drag force equals the net gravitational force upon the sphere. If the fluid is now set into solid-body rotation, the rising sphere has the same net gravitational force and hence the same drag as when the fluid is not rotating.

Because of the change in flow field caused by rotation, the sphere rises at a smaller velocity U' than when the fluid is not rotating. Thus, the Stokes drag $6\pi\rho\nu aU'$, with which all drags are non-dimensionalized, is smaller when the fluid is rotating than when it is not.

If we form the non-dimensional drag in the rotating case, $D/6\pi\rho\nu aU'$, we find that, although the drag itself is the same as the non-rotating case, because the Stokes drag is smaller, the dimensionless drag is increased by rotation.

The drag measurement without rotation is thus a calibration run that tells us the drag on the sphere. It is possible that the net gravitational force could be measured directly, but the accuracy required is greater than can be obtained simply by conventional techniques. The present method has the added advantage of allowing calibration checks to be made at frequent intervals during any one experiment.

Since an experiment cannot be performed in a fluid of infinite extent, a method must be devised to produce results for an infinite fluid in a finite-sized container. In this work, the sphere is allowed to rise through three cylinders of different diameters. The time of rise is found for each cylinder, and the results

extrapolated to a container of infinite size; or, more precisely, the rise-time is plotted versus a/Λ and extrapolated to the zero value of a/Λ, where Λ is the cylinder radius. In this way, the effect of finite R, T and a/Λ can be included in the final results.

3. Apparatus and procedure

The experimental equipment, although basically very simple, incorporates several interesting features. Figure 1 shows the major apparatus.

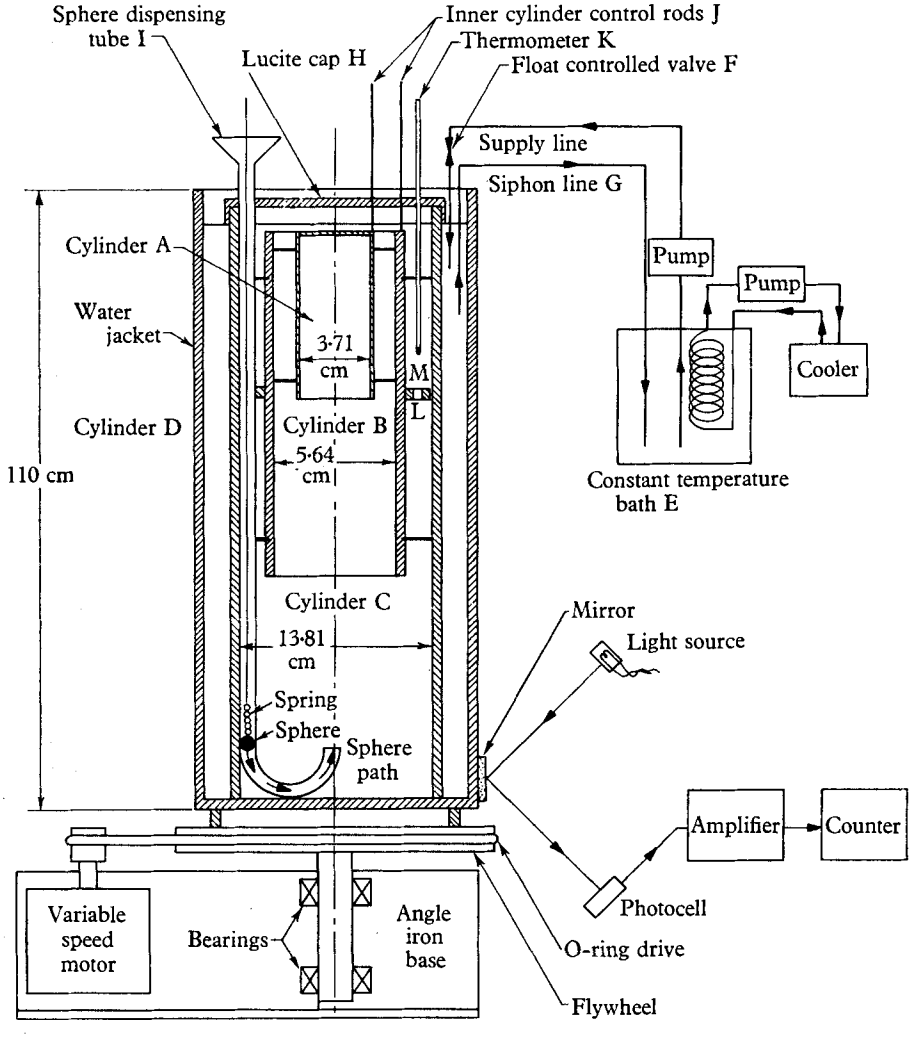

FIGURE 1. Apparatus.

The space between the two outer Lucite cylinders C and D is a constant-temperature water jacket. Water is pumped from a Fisher Isotemp bath E through a float valve F into the annular space, from when it is withdrawn by the siphon tube G back into the Isotemp bath. The temperature is controlled to with-

in $\pm$ 0·01 °C by this procedure. Such exact temperature control is quite essential for the accurate operation of the whole system. A 0·1 °C difference in temperature can cause the time of rise of the sphere to change by as much as 1 %, and this change, when the small difference in rise time caused by rotation is being measured, can result in inaccuracies of the order of 10 % in the over-all results.

The cylinder C holds the working fluid, glycerin. It is covered by a Lucite cap H, through which the sphere dispensing tube I, the inner-cylinder control rods J, and thermometer K protrude. Both inner cylinders A and B can be manipulated from outside by the control rods J. The larger of the two inner cylinders made of Lucite, has a simple pumping device attached to its middle. A Lucite annulus L has several holes cut in it; these are normally covered by a thin metal sheet M which can ride up and down on short support rods. When the inner tubes are moved up and down in the tube C, this device acts as a simple lift pump to circulate the glycerin and to make sure that it is well mixed so that no temperature gradients exist to alter the rise-time of the sphere.

Lines, 20 cm apart, are scribed on the outer cylinder. The time taken for the sphere to travel between the marks was measured to $\pm$ 0·05† sec using a stopwatch. The period of rotation of the cylinders was measured by reflecting light from a mirror into a photocell. The pulses created were sent into a counter that measured the time interval between them.

An operating procedure was devised to remove, as far as possible, the sources of error. Calibration and rotation tests were run in pairs, with the inner tubes in each of four possible positions. If we denote the smaller movable tube by the letter A, the larger movable tube by B, the outer fixed tube by C, and denote their relative position from the bottom by a sequence like CAB, this means that the sphere first moves through the cylinder C, then enters A, and finally B.

All tests used the following sequence: the speed of rotation was set at a particular value and the tubes were placed in position ABC. A calibration test was followed by two rotation tests and another calibration test. Then this sequence of tests was repeated for the tube positions BAC, CAB, CBA. Next the speed of rotation was changed and the whole procedure repeated. Four changes in rotation speed were made for each ball diameter and glycerin temperature used. Tests were run with ball diameters 0·254, 0·553 and 1·270 cm and glycerin temperatures 74, 84, 94 and 108 °F. It was necessary to carry out such a large number of experiments in order to cover completely the ranges of the parameters T, R and a/Λ.

The differential rotation ω between the sphere and the basic flow was found by feeding the output of the photocell into a Strobatac Light Source. The sphere could be viewed at the same position during each revolution of the outer cylinder. A small identifying mark was painted on the sphere, and the number of container revolutions needed for the sphere to make $\frac{1}{4}$ revolution relative to the basic solid-body rotation was determined.

† Found by 'calibrating' the observer against a known, repeatable time interval.

4. Reduction of data

The data collected were for different T and R in each case. However, we shall present curves for constant values of these two parameters and show how they compare with the theoretical predictions for the same constant values. For each ball diameter and constant temperature, curves of $1/U$ *vs.* a/Λ for the actual experimental values of T were plotted. A cross-plot of $1/U$ *vs.* T for various chosen, constant values of a/Λ was made. In particular, the value of $1/U$, i.e. $1/U_0'$, for $a/\Lambda = 0$ and $T = 0$ was found by extrapolation. The Reynolds number

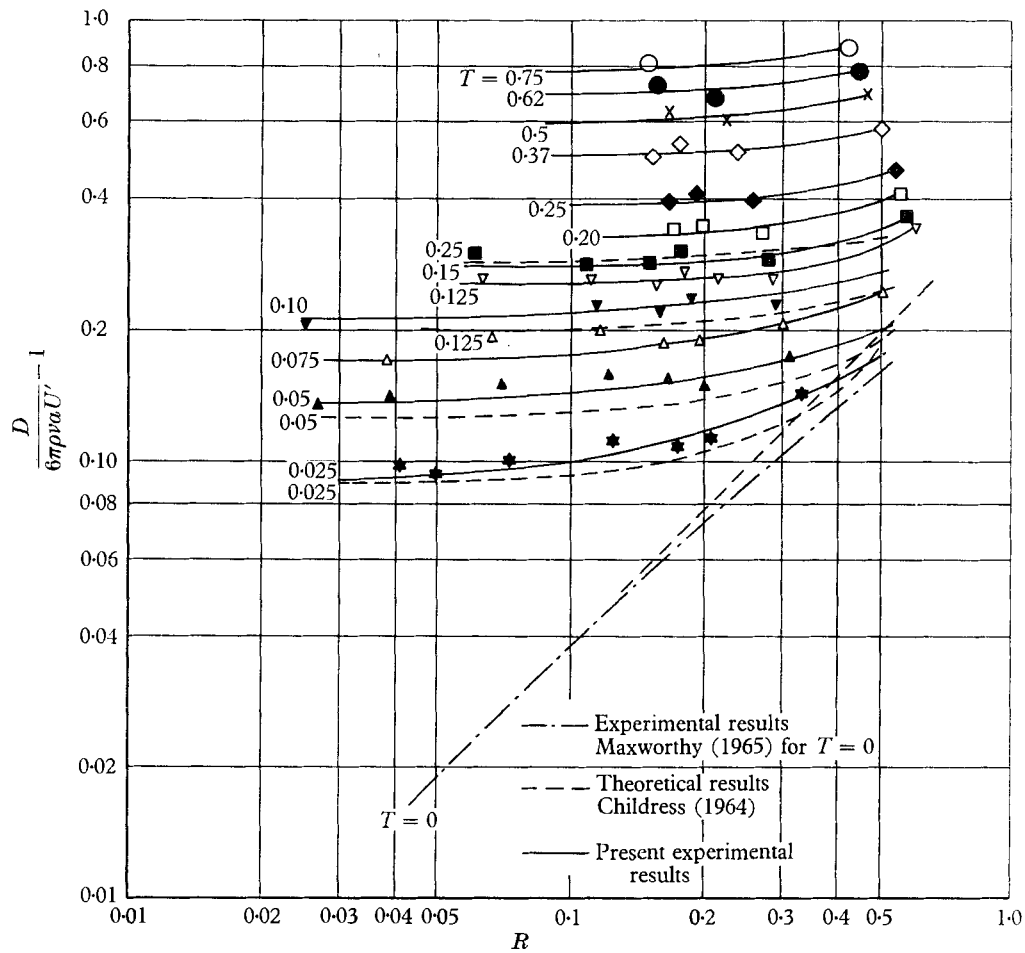

FIGURE 2. $D/6\pi\rho\nu aU' - 1$ *vs.* Reynolds number for various Taylor numbers.

R_0' of this point was calculated, and the sphere drag was found from the experimental values of Maxworthy (1965). This value is used as the calibration drag value D for the particular sphere and fluid temperature considered.

From these curves, values of $1/U$ were tabulated for various conveniently chosen constant values of T and for the constant values of a/Λ chosen earlier. Values of R for each of these points were calculated, together with values of $D/6\pi\rho\nu aU$ with rotation.

A further series of cross-plots of $D/6\pi\rho\nu aU$ *vs.* R for the various constant values of T was made, each set of curves being for a particular value of a/Λ. The points on these final plots contain all sources of error, both errors in original measurement and errors in extrapolation of these basic data.

The main source of the inaccuracy of about $\pm 2\,\%$ is due to the difficulty experienced in extrapolating the calibration curves to zero a/Λ. It is possible to reduce this arbitrary extrapolation to a certain extent. At the same time, this technique gives the effect of the wall and finite R on drag and can be compared with the

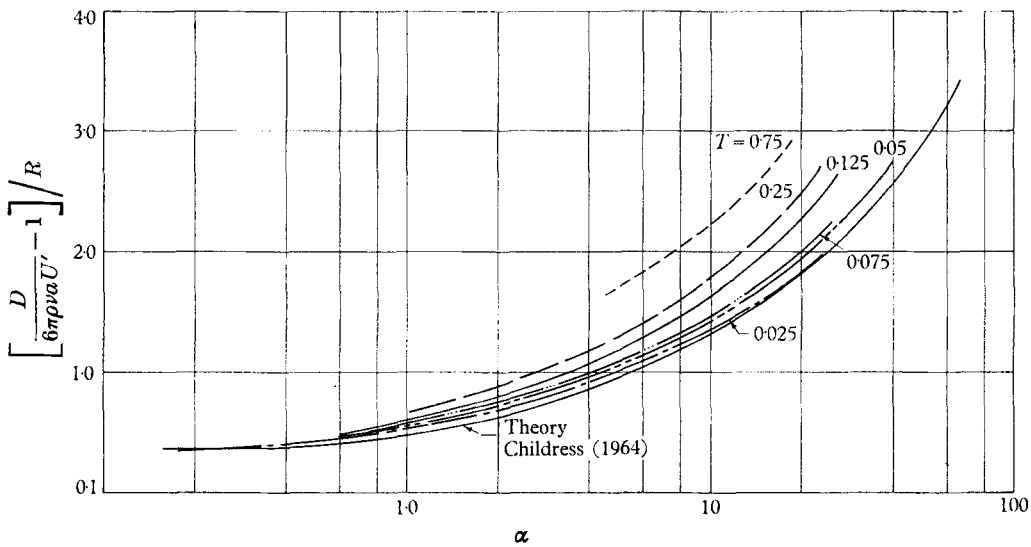

FIGURE 3. $[D/6\pi\rho\nu aU'-1]/R$ *vs.* α for various Taylor numbers.

theory of Faxen (1922). Extrapolation of the results with applied rotation are easier to perform since at low values of a/Λ they are almost constant and the inaccuracies of extrapolation correspondingly reduced; for them the following complicated technique was not used.

Extrapolated curves for the small-sphere diameters are almost straight, and are easy to extrapolate unambiguously; they are used as a starting point in a technique that builds curves for larger-sphere diameters, using the following 'bootstrap' technique.

The experimental curves of $1/U_0$ *vs.* a/Λ for each fluid temperature and the smallest sphere were plotted and extrapolated to zero a/Λ as almost straight lines. The non-dimensional drag $D/6\pi\rho\nu aU_0'$ at zero a/Λ was found from Maxworthy (1965). The drag and Reynolds number for each of the experimental points could then be calculated from the knowledge of D, U_0, a, ρ, and ν at each of these points. We now have curves of $D/6\pi\rho\nu aU_0$ *vs.* a/Λ for constant values of temperature, so that R varies monotonically along each of the curves in a known way. Since we wished to present graphs for constant values of R, it was necessary to interpolate between the experimental values at suitably chosen values of R. $D/6\pi\rho\nu aU_0$ was plotted versus the experimental values of R and constant

values of a/Λ. Values of the drag at chosen values of R could be found graphically at each value of a/Λ, and the original curve replotted as $D/6\pi\rho\nu aU_0$ *vs.* a/Λ for constant values of R. It is evident that when we repeat this procedure and

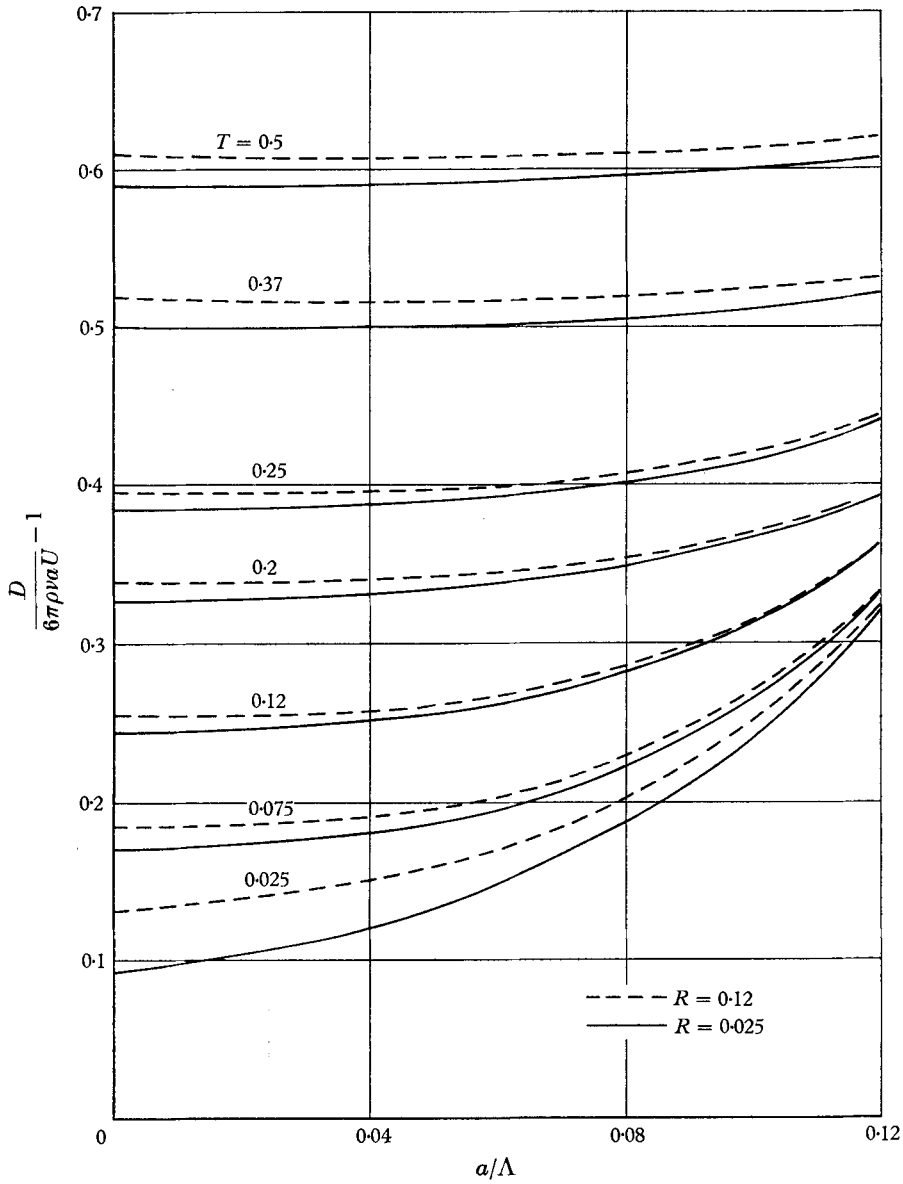

FIGURE 4. $D/6\pi\rho\nu aU - 1$ *vs.* a/Λ for various Taylor and Reynolds numbers.

extrapolate the curves obtained for larger sphere diameters, they must match these initial, small a/Λ curves.

Several trial extrapolations of the next larger sphere results were made until an extrapolation was found which closely matched the curves for the smallest spheres. The same procedure was followed for the still larger spheres except that

the extrapolation was now made to match the two previously coincident curves. The final curves show how the sphere drag varies for constant values of R and the complete range of a/Λ considered experimentally.

5. Results

Figures 2 and 3 show two convenient ways of presenting the experimental results. The first of $D/6\pi\rho\nu aU' - 1$ *vs.* R for various T up to 0·75 (with the wall effects removed) shows the modification of classical sphere drag and indicates good agreement between experiment and the theory of Childress (1964) when T and R are small; a continuous divergence exists as these two parameters increase. Of particular interest is the modification of the Reynolds-number dependence as the Taylor number is increased. When T is large, say $O(1)$, the

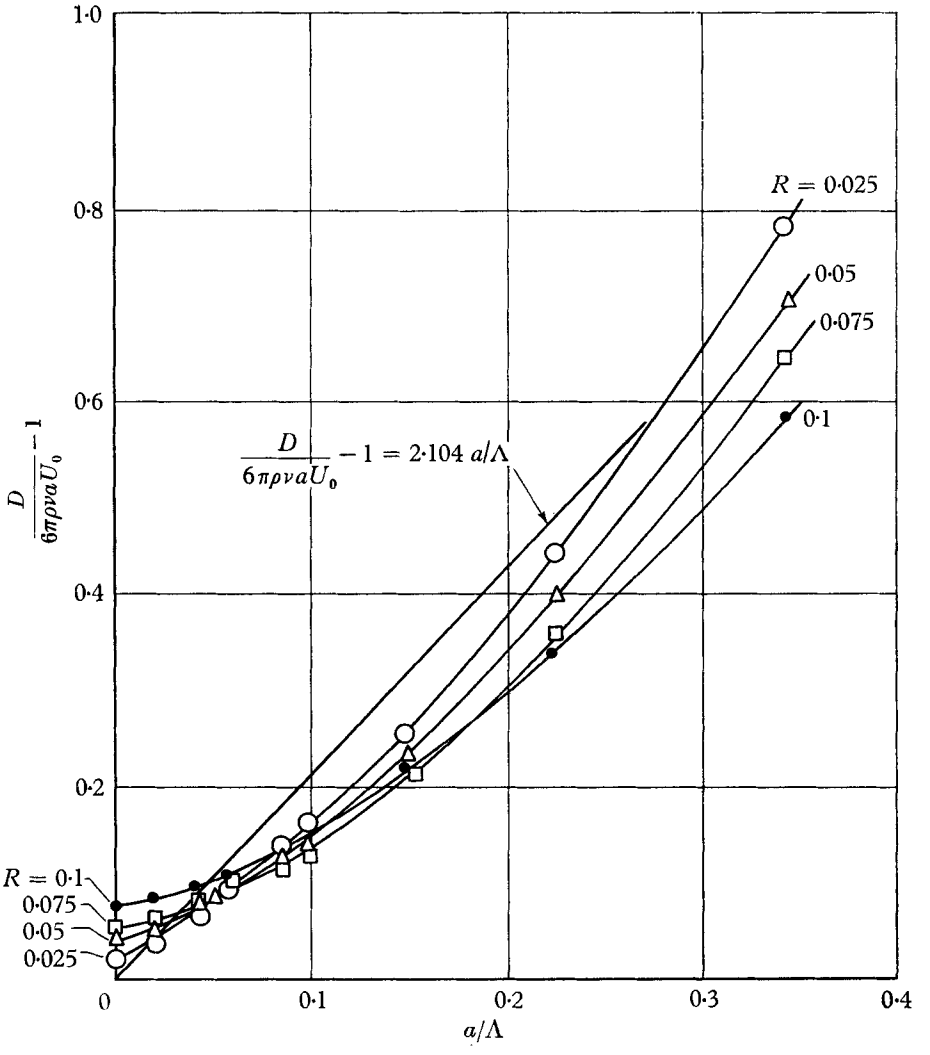

FIGURE 5. $D/6\pi\rho\nu aU_0 - 1$ *vs.* a/Λ for various Reynolds numbers with no rotation.

R dependence virtually disappears, until R is quite large. The result, though not unexpected, gives estimates of the magnitudes of the various terms in the equation of motion and allows one to make reasonable approximations to this equation when any one of the parameters becomes larger than any other.

In order to compare results more directly with the calculations of Childress (1964), $[D/6\pi\rho\nu aU' - 1]/R$ *vs.* α is plotted in figure 3, where $\alpha = 2T/R^2$. In this representation Childress's results reduce to the single curve shown. One feature of the theory is missing; the small decrease in drag predicted at low values of α does not seem to be indicated by the experiments, although the experimental range is not large enough for the possibility to be rejected completely.

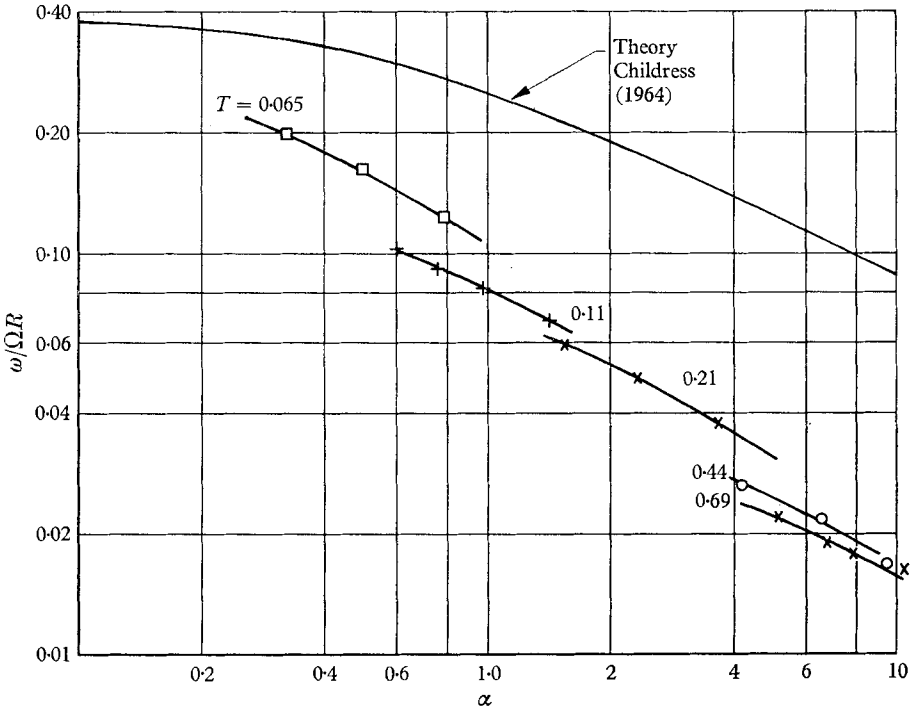

FIGURE 6. $\omega/\Omega R$ *vs.* α for various Taylor numbers.

All of the results presented so far have been concerned with drag in an infinite medium. The experimental technique also allows the determination of the effects of fluid containment within a cylinder. Figure 4 shows $D/6\pi\rho\nu aU - 1$ as ordinate, a/Λ as abscissa, and T and R as parameters. Only a few of the resulting curves were plotted in order to reduce the confusion that could result from putting all of the possible curves on one presentation.

The only set of data which could not be reduced accurately by this method was that for the curves $T = 0$. These are plotted in figure 5, using the technique described in § 4.

Measurements of the rate of differential rotation are shown in figure 6 where $\omega/\Omega R$ is plotted versus α. Here agreement with theory at low T is apparently not good and requires explanation.

6. Discussion

6.1. *Motion in a fluid of infinite extent*

Stated succinctly, the results of these experiments are: rotation greatly increases, and plays the major role in determining the drag on a sphere moving through a rotating viscous fluid. The very dominant role of the Coriolis parameter, even when R and T are of the same magnitude, requires some discussion.

The most reasonable consistency argument is as follows: writing the non-dimensional equation of motion in terms of the vorticity, one obtains:

$$\nabla^2\boldsymbol{\omega} + \operatorname{curl}[\mathbf{U} \times \{R\boldsymbol{\omega} + 2T\mathbf{i}\}] = 0, \tag{1}$$

where $\boldsymbol{\omega}$ and $\mathbf{U}$ are the non-dimensionalized vorticity and velocity vectors, respectively, and $\mathbf{i}$ the unit vector in the direction of the applied rotation. Because of the action of the Coriolis forces, all three vorticity components, ω_z, ω_r, and ω_ϕ must be considered in a convenient cylindrical co-ordinate system, z, r, ϕ. Note that in ordinary small-R flow, only ω_ϕ exists.

Rotation has two effects: it modifies the magnitude and distribution of ω_ϕ that would have existed in its absence, and it produces new components ω_z and ω_r, the magnitudes of which depend in some way on the magnitude of the applied rotation. When R and T are of about the same magnitude, the experiments indicate that the drag and presumably the flow field are determined mainly by a balance of Coriolis and viscous forces. From equation (1) this means that, under these circumstances, $\boldsymbol{\omega}$ is smaller than $2\mathbf{i}$. This conclusion is consistent with the physical intuition we have developed about such flows, for it seems unlikely that ω_z, for example, could be magnified to the extent that it might exceed the magnitude of the applied vorticity.

A self-evident benefit of this conclusion is the possibility of producing valid theories for any T, without having to worry about the non-linear convective terms in the equation of motion unless R is at least of the same order as T. It is possible that large-T theories will then give good representation of the real situation, even when R is large but smaller than T.

It is one of the definite conclusions of this work and of Maxworthy (1965) that the theoretical first-order corrections to Stokes's drag, caused by both rotation and finite R, are quite adequate to describe accurately the real flow over a reasonable range of parameter values. This is even more interesting because they are accurate even where higher-order terms could be expected to produce corrections that would be very apparent to the scale considered. This can be seen very clearly in Maxworthy (1965) where a case is considered for which some of the higher-order terms are available.

An apparently large discrepancy between the theoretically-predicted differential sphere rotation and the measured values requires explanation. If one cross-plots the raw data curves to see how the differential rotation varies with T, it is found that the extrapolation to zero T, although changing very rapidly, is not completely ridiculous. Thus, while the drag varies slowly as T approaches zero, the differential rotation varies very rapidly.

6.2. *Motion in a fluid of finite extent*

The wall effects are decreased by rotation. The effect of the Coriolis force on flow past a body is to decrease the radial velocity of flow around it. In the limit of large T, the radial velocity is completely suppressed, and the flow, the so-called cylindrical or 'slug' flow, is the same in all planes perpendicular to the axis of rotation (Taylor 1923). This constraint on the radial flow, tending to straighten the streamlines, means that the straightening effect of the walls of the cylindrical container is reduced. In the limit of large T, when the flow is wholly one-dimensional, the walls can have no effect at all, since the flow streamlines, having no curvature in the meridional plane, are not aware of the presence of the wall. Figure 4 shows that rotation also has the effect of uncrossing the lines of constant R, at least for values of a/Λ below 0·12.

6.3. *Similarity to magneto-fluid dynamic flows*

The prediction of magneto-fluid dynamic (M.F.D.) effects from similar effects in a rotating fluid was one of the original purposes of the present work. Although no analogy exists in the strictest sense, the similarity is interesting enough to warrant attention. The present discussion will be limited to a few simple remarks on the low R, low T, low H^2 cases, where H^2, the square of the Hartman number, is the ratio of magnetic forces to viscous forces and is the quantity analogous to the Taylor number.

In M.F.D., in addition to the presence of a magnetic field, an extra material property is present, the electrical diffusivity $1/\mu\sigma$, where σ is the electrical conductivity and μ the permeability of the fluid medium. Thus, one further dimensionless parameter can be formed; namely, the magnetic Prandtl number $\nu\mu\sigma$, the ratio of viscous-diffusivity to magnetic diffusivity. The electrical diffusivity dissipates azimuthal electric current; while in the rotating flow, viscous diffusivity dissipates the azimuthal swirl velocity. Thus, for the two cases to be similar, strictly we can only consider the case of $\nu\mu\sigma = 1$.

Although the equations to be solved in the two cases are rather different, a sixth-order equation in the rotating case and a fourth-order in the M.F.D. case, the methods of analysis for both are virtually identical and point to the importance of the parameters $T^{\frac{1}{2}}/R$ and H/R. Superficially, these two parameters would seem to have no great physical significance, and, in fact, they have been rather neglected in favour of the combinations T/R and H^2/R, which measure the relative magnitudes of Coriolis or Lorentz forces to inertia forces. Childress has shown the mathematical significance of both the former, and their physical importance is just being realized (Goldberg & Jarvinen 1964). They can be found in a natural way by calculating a Reynolds number based on a length over which the Coriolis or Lorentz forces are of comparable magnitude to viscous forces; e.g. $L \sim [\nu/\Omega]^{\frac{1}{2}}$; $L \sim [\rho\nu^2/\mu]^{\frac{1}{2}}/B$, where B is the magnetic field strength. Since most of the dissipation takes place in regions where this criterion is satisfied, the appearance of these parmeters is not surprising.

Under the circumstance considered, it is proposed that the available M.F.D. theories will adequately describe low R, low H flows. The appearance of $\nu\mu\sigma$

as an independent parameter restricts the usefulness of the comparison, but it is believed that confidence can be placed in the results even when $\nu\mu\sigma$ is not unity.

The workmanship and design abilities of Mr D. E. Griffith have been of inestimable value in this experimental investigation. Many fruitful discussions with Dr W. S. Childress and Dr P. G. Saffman are also gratefully acknowledged.

This paper presents the results of one phase of research carried out at the Jet Propulsion Laboratory, California Institute of Technology, under Contract no. NAS 7-100, sponsored by the National Aeronautics and Space Administration.

REFERENCES

CHILDRESS, W. S. 1963 Rotating viscous flow past an axially symmetric solid. *Space Programs Summary* 37–18, vol. IV, p. 46. Jet Propulsion Laboratory, Pasadena, California.

CHILDRESS, W. S. 1964 The slow motion of a sphere in a rotating, viscous fluid. *J. Fluid Mech.* **20**, 305.

FAXEN, H. 1922 Dissertation. Uppsala University, Sweden.

GOLDBERG, A. & JARVINEN, P. O. 1964 *AVCO Everett Research Laboratory Research Note* no. 415.

MAXWORTHY, T. 1965 Accurate measurements of sphere drag at low Reynolds numbers. *J. Fluid Mech.* **23**, 369.

SQUIRE, H. B. 1956 Rotating Fluids. *Surveys in Mechanics*, p. 139. Ed. G. K. Batchelor & R. M. Davies. Cambridge University Press.

TAYLOR, G. I. 1923 The motion of a sphere in a rotating fluid. *Proc. Roy. Soc.* A, **102**, 180.